

## Axial Ratio Enhancement of Equilateral Triangular-Ring Slot Antenna Using Coupled Diagonal Line Slots

Asif Awaludin<sup>1, 2, \*</sup>, Josaphat T. S. Sumantyo<sup>1</sup>, Cahya E. Santosa<sup>1, 2</sup>,  
and Mohd Z. Baharuddin<sup>3</sup>

**Abstract**—Wideband circularly polarized antenna is required for many satellite applications. Circularly polarized (CP) Equilateral Triangular-Ring Slot (ETRS) antenna has narrow 3-dB axial ratio bandwidth (ARBW) compared to its impedance bandwidth. Two diagonal line slots were introduced to ETRS for enhancing its 3-dB ARBW. The diagonal line slots were inserted on the left and right side of ETRS. Lengths of the left and right line slots correspond to the lowest and highest frequencies of ETRS antenna 3-dB ARBW, respectively. Both diagonal line slots have successfully improved 3-dB ARBW of ETRS antenna by achieving 680 MHz or 37% fractional bandwidth. Measured results of  $x$ - $z$  and  $y$ - $z$  planes of radiation patterns also confirm that the antenna has bidirectional radiation and presents good CP performance within its 3-dB ARBW. ETRS antenna RHCP gain is also improved thanks to the diagonal line slots insertion.

### 1. INTRODUCTION

Many satellite applications, such as Global Navigation Satellite System (GNSS) and L-band satellite communication system, require wideband CP antenna. This antenna is widely utilized for satellite applications thanks to their resilience to polarization mismatch, multi-path interferences and Faraday rotation effect. CP printed-slot antennas have been broadly developed to achieve wide 3-dB ARBW thanks to its compact size, light weight and simple fabrication method. Based on type of feed line, printed-slot antennas can be categorized into CPW-fed and microstrip-line-fed antennas. A CPW-fed antenna usually has wider CP bandwidth but with lower gain than a microstrip-line-fed antenna. A CPW-fed slot antenna with lightening feed line and inverted-L grounded strips [1] provides 48% 3-dB ARBW and 4.2 dBic peak gain, whereas a CPW-fed symmetric-aperture [2] antenna presents broader 3-dB ARBW (68%) and 4 dBic peak gain. Meanwhile, several types of microstrip-line-fed ring slot antennas have lower bandwidth and gain, such as square ring slot [3, 4] and annular ring slot [4]. However, wider ring slot incorporated with grounded hat-shaped patches and a bent feed line has significantly improved annular ring slot [5] by recording 65% 3-dB ARBW and 5.1 dBic peak gain. Better gain performances are presented by microstrip-line-fed wide slot antennas, such as a T-shaped slot [6] antenna (12% 3-dB ARBW and 5.5 dBic peak gain) and L-shaped microstrip-fed printed circular-shaped slot [7] antenna (44% 3-dB ARBW and 5 dBic peak gain). Meanwhile, an equilateral triangular-ring slot [8] antenna excited with protruded L-shaped strip feed line has achieved 3.2% 3-dB ARBW and 3.4 average gain. CP bandwidth and gain improvement of this antenna are obtained by moving its inner triangular patch to the upper side acting as triangular parasitic patch for a wide slot antenna. As a result, 31% 3-dB ARBW and 6.7 average gain are achieved. However, the drawbacks are much bigger size and weaker structure.

---

Received 25 October 2016, Accepted 6 December 2016, Scheduled 28 December 2016

\* Corresponding author: Asif Awaludin (asif@chiba-u.jp).

<sup>1</sup> School of Advanced Integration Science, Center for Environmental Remote Sensing, Chiba University, Chiba, Japan. <sup>2</sup> National Institute of Aeronautics and Space (LAPAN), Jakarta, Indonesia. <sup>3</sup> Universiti Tenaga Nasional, Putrajaya, Malaysia.

Conventional ring slot antennas are linearly polarized. Therefore, modification on the structure such as introducing perturbation to the slot, linking two slot rings [9], and hybrid coupler feed network [10, 11] are proposed to convert polarization from linear to circular [4]. However, these modifications yield narrower 3-dB ARBW than its impedance bandwidth. Thus, further 3-dB ARBW enhancement technique is necessary. Many methods have been implemented for this purpose, for example two hat-shaped perturbations inserted into annular-ring slot incorporated with bent feed line [5]. Meanwhile, utilization of diagonal line slot for improving CP radiation performance of patch antennas was presented in many articles, for instance square patch antenna with a diagonal slot [12], equilateral triangular patch antenna with a narrow horizontal slot [13], and circular patch with slanted rectangular slot [14]. On the other hand, employment of line slot to enhance 3-dB ARBW and improve gain of ring slot antenna has not been investigated. Utilization of two parallel edge slots to lower cross-polarization of linearly polarized v-slot has been reported [15], but it did not achieve any impedance or axial bandwidth improvement.

The goal of this study is to present a design for enhancing CP performance of ETRS to achieve wide 3-dB ARBW close to its impedance bandwidth. Since a conventional ETRS antenna is linearly polarized, CP radiation is generated by making several truncations and perturbation to the slot and introducing meandered feed line. The truncations are created by chamfering ETRS corners in equal sizes. An equilateral triangular patch with side lengths equal to chamfering size is inserted as a perturbation, while the feed line is deformed by introducing additional branch lines. Further, to improve 3-dB ARBW of the modified ETRS antenna, two different lengths of diagonal line slots are loaded into the antenna on the left and right sides of ETRS. Mutual coupling between the line slots and ETRS which result in generation of wider CP radiation bandwidth will be investigated by analyzing surface current distributions of the antenna. Further effects of mutual coupling that alter antenna radiation pattern and gain as addressed in [16] are examined as well.

## 2. CIRCULARLY POLARIZED ETRS ANTENNA

Conventional ETRS antenna as illustrated in Fig. 1(a) has linear polarization (LP) radiation. Resonant frequency of this antenna is determined by mean circumference of its ring slot which depends on the slot width  $w_r$  and slot side length  $R_1$ . The antenna is simulated on a substrate with a relative permittivity  $\epsilon_r$  of 2.17, thickness  $h$  of 1.6 mm and loss tangent of 0.0005. The antenna design and simulation are conducted using method of moments (MoM). Inner side length  $R_1$  of 18.3 mm and outer side length  $R_2$  of 101.4 mm create slot width  $w_r = \tan 30^\circ \times (R_2 - R_1)/2 = 24$  mm and mean side length  $R_m = (R_2 + R_1)/2 = 59.8$  mm. Thus, mean circumference of ETRS is  $3R_m = 179.5$  mm. These configurations with antenna width  $W = L = 130$  mm yield resonant frequency of 1.269 GHz. As a result, mean circumference of this resonant frequency is equivalent to  $0.89\lambda_g$ .

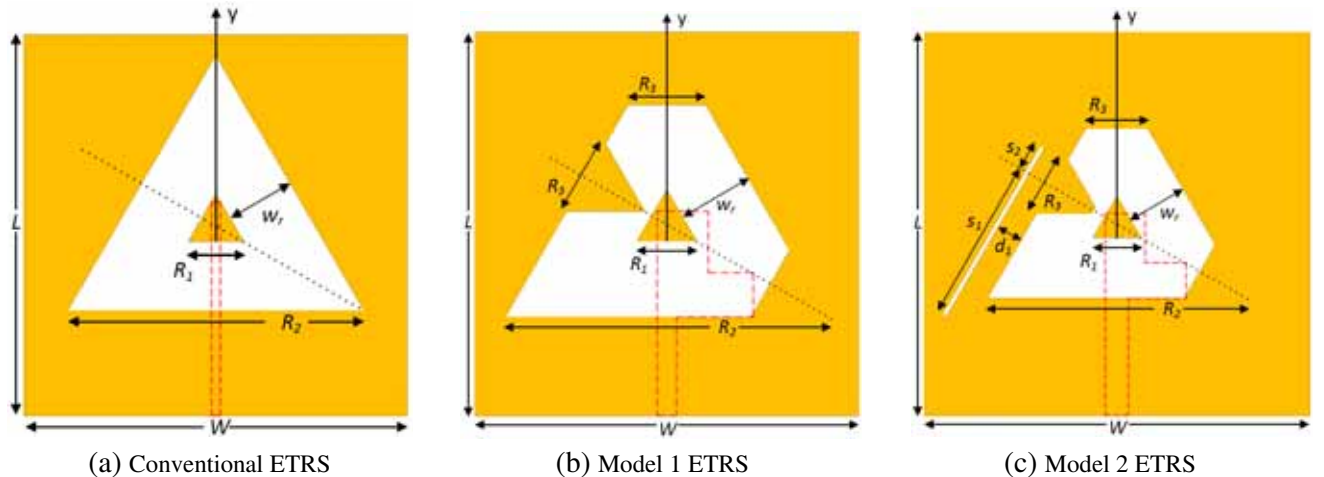


**Figure 1.** Geometry of (a) conventional model, (b) model 1 and (c) model 2 of ETRS antenna.

CP radiation can be produced from this LP antenna by modifying the slot structure and its feed line. Top and bottom left edges of the ETRS are truncated by  $R_3$  as depicted in Fig. 1(b). An equilateral triangular patch with length  $R_3$  is introduced into the patch as a perturbation. This perturbation insertion method has been applied also to annular and square ring slot antennas [4, 5]. The length of  $R_3$  influences antenna resonant frequency and axial ratio as it changes the slot size. Larger value of  $R_3$  reduces slot size, thus yields lower resonant frequency.  $R_3$  value for truncation and perturbation patch resulting in better (lowest) axial ratio is 24 mm. The modified ETRS is fed by deformed feed line which has 6 mm of width incorporated with upper and lower branches extending to the right (+ $x$  direction). The lower branch has length of 24 mm, and its bottom line is in line with the bottom line of ETRS, while the length of upper branch is 10 mm. The length of both branches are useful for adjusting the width of impedance bandwidth and center frequency of 3-dB ARBW. Proper adjustment is needed to synchronize center frequency of both bandwidths. Investigation on magnetic surface current distribution reveals that the truncations and perturbation patch generate more currents on the truncated areas (see Fig. 5(a)) yielding equitable distribution compared to the conventional model which has strong current mostly on the lower side of ETRS and very low current on the top side. This type of antenna is referred as model 1 ETRS antenna which achieves much wider impedance bandwidth than conventional one and generates CP operation at 1.727 GHz with 254 MHz of 3-dB ARBW.

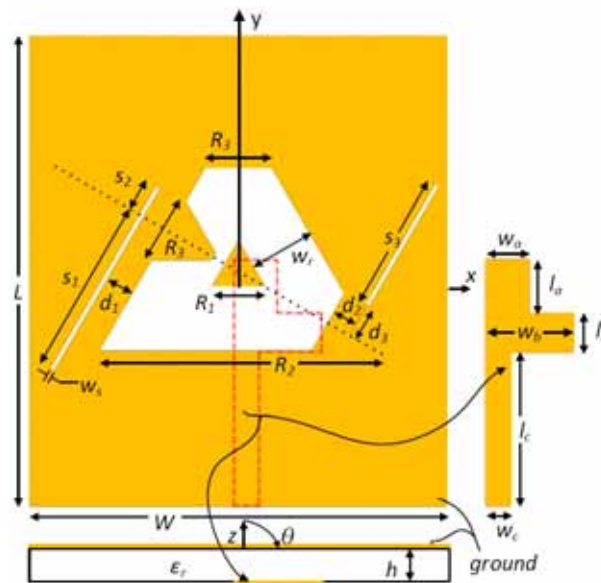


**Figure 2.** Geometry of expanded model 3 ETRS. Microstrip feed line is described in the right side and edge profile of the antenna is drawn in the bottom side.

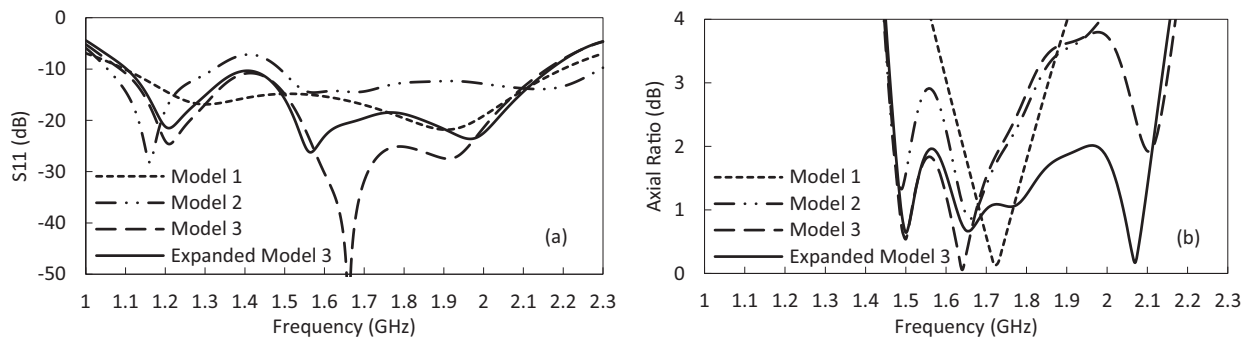


**Figure 3.** Comparison of (a)  $S_{11}$  and (b) axial ratio of model 1, model 2, model 3 and expanded model 3 of ETRS antenna.

### 3. COUPLED DIAGONAL LINE SLOTS FOR 3-DB ARBW ENHANCEMENT

#### 3.1. Lower Frequency Diagonal Line Slot (Model 2)

CP performance improvement of model 1 ETRS antenna is necessary as its 3-dB ARBW is much narrower than its impedance bandwidth. Diagonal line slot has been proven to produce two degenerate orthogonal modes for CP radiation of patch antenna [12]. A similar mechanism was implemented to model 1 to generate another resonant frequency with two equal-amplitude in-phase quadrature modes so as to broaden the 3-dB ARBW. This new design is referred as model 2 and outlined in Fig. 1(c). First resonant frequency of narrow line slot is similar to a magnetic dipole where the length is equal to  $0.5\lambda_g$  [17]. Thus the diagonal line slot inserted into the antenna also has resonant frequency corresponding to its length. Performance of the line slot is influenced by mutual coupling with ETRS which depends on the distance between centers of the two slots, slot length, and field distribution around the slot [18]. By considering that diagonal line slot achieves narrow 3-dB ARBW, resonant frequency of the left diagonal line slot should be approximately equal to the lowest frequency at 3-dB ARBW of model 1. The angle of diagonal line slot also determines its polarization. Angle of  $30^\circ$  provides better circular polarization.

As model 1 has the lowest frequency of its 3-dB ARBW at 1.6 GHz, the left line slot is designed for frequency around 1.6 GHz as well. Thus the length of the left line slot should be around 80 mm. The values of  $s_1$  and  $s_2$  with respect to dotted diagonal line, which contribute to slot length, and spacing  $d_1$  determine the mutual admittance between the diagonal line slot and ETRS. Therefore, proper tuning is critical to obtaining the best mutual coupling which can produce good axial ratio profile. Simulated results shown in Fig. 4(a) indicate that 80 mm of slot length, where  $s_1$  and  $s_2$  are 66.6 mm and 13.5 mm,

**Table 1.** Dimensions of ETRS antenna models.

Models	$L$ mm	$W$ mm	$w_c$ mm	$w_r$ mm	$R_1$ mm	$R_2$ mm	$R_3$ mm
Conventional	130	130	3	24	18.3	101.4	-
Model 1	120	120	6	24	18.3	101.4	24.3
Model 2	150	150	9	24	18.3	101.4	24.3
Model 3	150	150	9	24	18.3	101.4	24.3
Model 3 Expanded	170	150	9	24	18.3	101.4	24.3

**Table 2.** Performances of model 1, model 2, model 3 and expanded model 3 of ETRS antenna.

Models	$f_{cibw}$ MHz	Impedance Bandwidth MHz, %	$f_{carbw}$ MHz	3-dB ARBW MHz, %
Conventional	1269	1100–1438 338, 26.6%		
Model 1	1648.5	1097–2200 1103, 67%	1727	1600–1854 254, 14.7%
Model 2	1891	1488–2294 806, 42.6%	1642	1456–1828 372, 22.7%
Model 3	1623	1087–2159 1072, 66%	1634.5 & 2098	1458–1811 & 2048–2148 353, 21.6% & 100, 4.8%
expanded Model 3	1635	1102–2168 1066, 65.2%	1798	1461–2135 674, 37.5%
Measured expanded Model 3	1785	1390–2180 790, 44.3%	1840	1500–2180 680, 37%

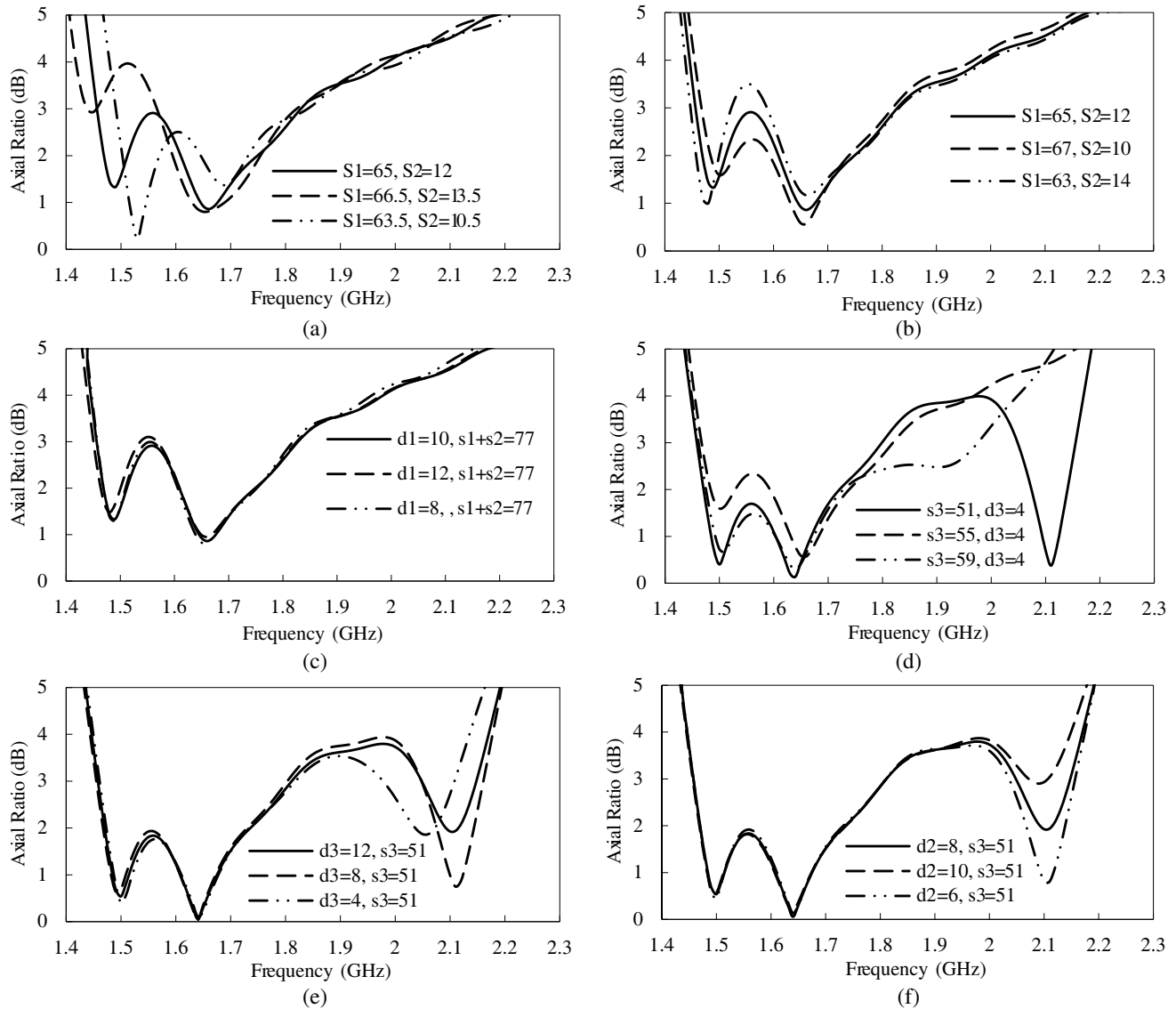


**Figure 4.** Comparison of diagonal line slot 3-dB ARBW by variation of (a) left line slot length with  $d_1 = 10$  mm for model 2, (b) left line slot height position with  $d_1 = 10$  mm for model 2, (c)  $d_1$  with left line slot length = 77 mm for model 2, (d) right line slot length with  $d_2 = 8$  mm for model 3, (e) right line slot height position with  $d_2 = 8$  mm for model 3, (f)  $d_2$  with  $d_3 = 12$  mm for model 3.

respectively, yields wider bandwidth, but the axial ratio values are above 3-dB, while 65 mm of  $s_1$  and 12 mm of  $s_2$  contribute to 77 mm of slot length produce narrower bandwidth, but its axial ratio values are under 3-dB. Shorter slot length results in much narrower axial ratio bandwidth. Height position of the line slot created by change on  $s_1$  and  $s_2$  size as shown in Fig. 4(b) is also critical. Higher positions than 65 mm of  $s_1$  and 12 mm of  $s_2$  increase the bandwidth but move axial ratio values inside the bandwidth to above 3-dB. Conversely, lower position has opposite impact. Meanwhile, the change of  $d_1$  distance by 2 mm closer or farther slightly raises the axial ratio to higher (worst) values as illustrated in Fig. 4(c). Feedline of model 2 is also adjusted with  $w_c$  set to 9 mm, whereas the lengths of lower and upper branches are tuned to 22.5 mm and 6.5 mm, respectively.

After several adjustments, 77 mm of left line slot length with  $s_1 = 65$  mm,  $s_2 = 12$  mm, and  $d_1 = 10$  mm has recorded better performance. These configurations result in 1.45–1.79 GHz bandwidth of axial ratio for model 2 antenna as shown in Fig. 3 and summarized in Table 2. Surface current

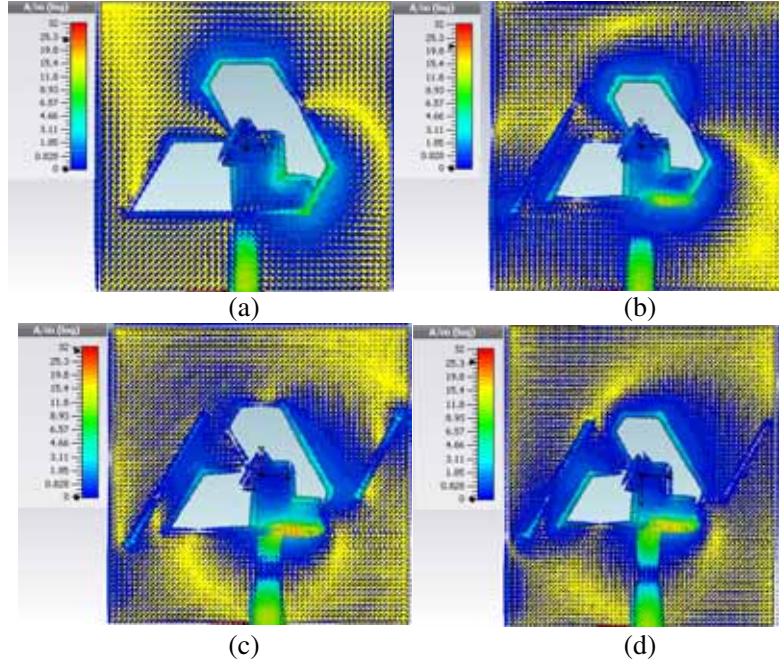


**Figure 5.** Surface current distributions at 1.8 GHz performed by (a) model 1, (b) model 2, (c) model 3 and (d) expanded model 3 of ETRS antenna.

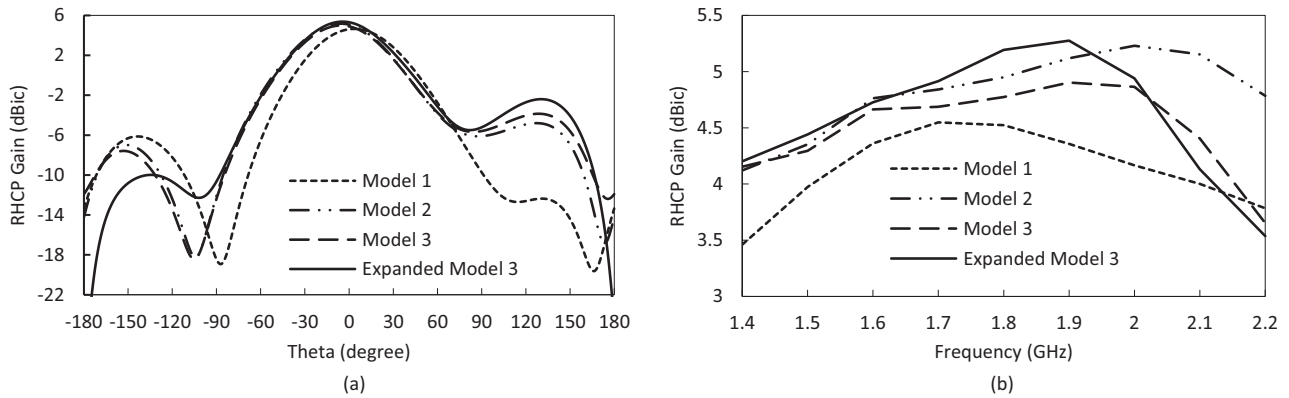


**Figure 6.** Comparison of (a) gains and (b) radiation patterns at 1.8 GHz performed by model 1, model 2, model 3 and expanded model 3 of ETRS antenna.

distribution shown in Fig. 5(b) indicates that mutual admittance between the two slots has attracted more surface current to the left line slot than in model 1 for generating two degenerate orthogonal modes of CP operation. Insertion of the left line slot to the antenna has successfully widened 3-dB ARBW of model 2 to the lower frequency by recording improvement of 118 MHz or 8% more than model 1. Mutual coupling of the two slots has altered radiation pattern of the antenna as discussed in [16]. Introduction of left line slot has shifted the direction of main beam from  $4^\circ$  by model 1 to  $-6^\circ$  by model 2. RHCP gain has also been improved by the left line slot. Model 1 has recorded 4.55 dBic at 1.7 GHz, while model 2 has achieved 4.84 dBic at 1.7 GHz and 5.23 dBic at 2 GHz. Radiation patterns and gains of model 1 and model 2 are depicted in Fig. 6(a) and Fig. 6(b), respectively.

### 3.2. Higher Frequency Diagonal Line Slot (Model 3)

Further 3-dB ARBW enhancement of model 2 is realized by inserting another  $30^\circ$  diagonal line slot on the right side of ETRS close to the truncation area, denoted as model 3. Resonant frequency of the right line slot is set at around the highest frequency of 3-dB ARBW which is 1.828 GHz. However, since the axial ratio reaches 4 dB at 2.16 GHz which is far from 1.828 GHz, it is encouraging to try to widen 3-dB ARBW from this point. Thus the length of the right line slot is adjusted to be around  $0.5\lambda_g = 59$  mm. Mutual coupling between the right line slot and ETRS depends on slot length  $s_3$ , spacing  $d_2$ , and distance  $d_3$ . Fig. 4(d) shows that right line slot length of 59 mm, manifested by 59 mm of  $s_3$  and 4 mm of  $d_3$ , with  $d_3 = 8$  mm has successfully enhanced 3-dB ARBW recorded by model 2 to be 520 MHz or 30% fractional bandwidth with 1720 MHz of 3-dB ARBW center frequency. Further, shortening  $s_3$  will improve axial ratio bandwidth.  $S_3$  of 51 mm with 12 mm of  $d_3$  generates two parts of 3-dB ARBW where a new part appears at 2.1 GHz as depicted in Fig. 3 and summarized in Table 2. In order to obtain wide single 3-dB ARBW, its axial ratio values need to be lowered below 3-dB. For this purpose, some adjustments by changing  $d_2$  and  $d_3$  distances with fixed  $s_3$  of 51 mm have been conducted. Decreasing  $d_3$  distance, which means moving the line slot to a lower position, will decrease the bandwidth, as illustrated in Fig. 4(e), while decreasing or increasing  $d_2$  distance has little impact on the dual band profile, as highlighted in Fig. 4(f). Therefore,  $d_2$  and  $d_3$  are maintained to be 8 mm and 12 mm, respectively. Feedline dimension of model 3 is similar to model 2, but its position shifts 3 mm to  $+x$  direction.

Mutual coupling attracts surface currents to peripheral area of the right line slot and decreases current on the top right side of the antenna to provide another two equal-amplitude in-phase quadrature modes (see Fig. 5(c)). Insertion of right line slot has slightly shifted direction of model 2 main beam by  $-1^\circ$ . RHCP gain has dropped to 4.7 dBic at 1.7 GHz and 4.9 dBic at 1.9 GHz due to this insertion. Radiation pattern and gain of model 3 are illustrated in Fig. 6(a) and Fig. 6(b), respectively.

### 3.3. Antenna Length Expansion (Model 3 Expanded)

Efforts to integrate two parts of 3-dB ARBW produced by model 3 for obtaining wide single 3-dB ARBW by adjusting  $d_2$  and  $d_3$  distances have been unsuccessful. This problem can be tackled by expanding length  $L$  of the antenna ground by considering that it must yield  $\lambda/4$  delay to the feed line as well. Simulated surface current distribution indicates that extension by 10 mm to  $+y$  direction and 10 mm to  $-y$  direction have been able to provide  $\lambda/4$  delay to the feed line, while extending feed line without ground plane extension resulting in no significant improvement. The new design is referred as expanded model 3 as depicted in Fig. 2. Dimensions of all ETRS models are tabulated in Table 1. The extended ground length has increased the currents distributed on the top side of ETRS to improve 90-degree phase difference which can be seen in Fig. 5(d). As a result, wide single 3-dB ARBW performance which covers frequency range 1.461–2.135 GHz is obtained, as depicted in Fig. 3 and summarized in Table 2. Antenna length extension has slightly moved direction of model 3 main beam by  $-1^\circ$ , as illustrated in Fig. 6(a). Improvement of RHCP gain has been recorded by providing 4.9 dBic at 1.7 GHz and 5.28 dBic at 1.9 GHz thanks to this extension, as depicted in Fig. 6(b).

## 4. MEASURED RESULTS AND DISCUSSIONS

Simulated expanded model 3 ETRS antenna must be verified to confirm the results. For this purpose, expanded model 3 was manufactured (see Fig. 7) and measured using RF Vector Network Analyzer (Agilent, E5062A, ENA-L) in anechoic chamber. Fig. 8(a) highlights that the fabricated antenna shows an impedance bandwidth in good agreement with the simulated model. Simulated results indicate that reflection coefficient reaches close to  $-10$  dB at 1.41 GHz, while its measured results cross the same value at 1.39 GHz to record 790 MHz of impedance bandwidth from 1.39 to 2.18 GHz. CP performance of the manufactured antenna also conforms the simulated model as illustrated in Fig. 8(b). 3-dB ARBW presented by fabricated antenna records 680 MHz of bandwidth from 1.5 to 2.18 GHz similar to the simulated one. This 3-dB ARBW is located entirely in the impedance bandwidth coverage. Thus, the fabricated antenna generates CP operation with similar center frequency and bandwidth to its 3-dB ARBW, as summarized in Table 2.

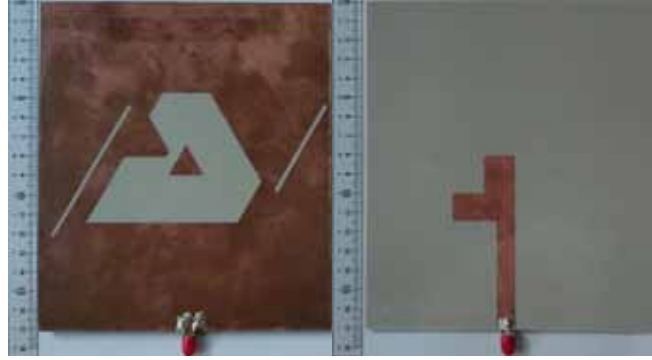


**Figure 7.** Photograph of fabricated expanded model 3 ETRS antenna.

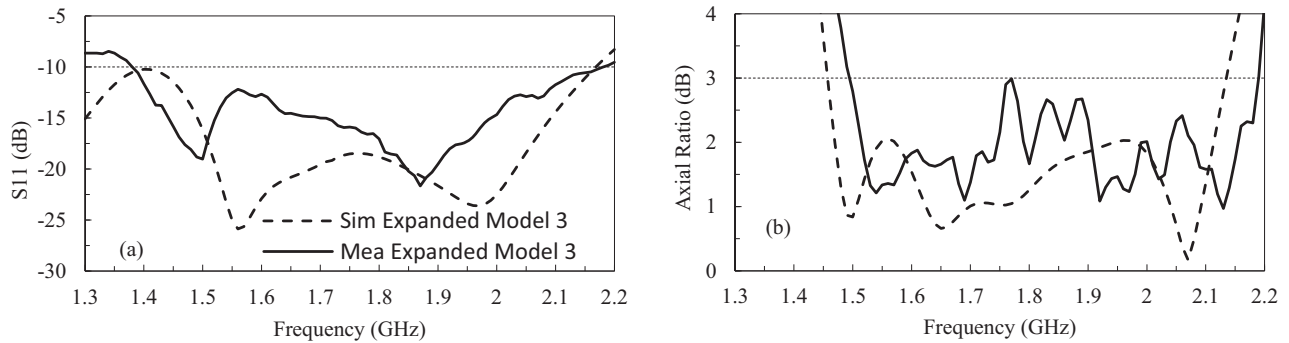


**Figure 8.** Simulated and measured (a)  $S_{11}$  and (b) axial ratio of expanded model 3 of ETRS antenna.

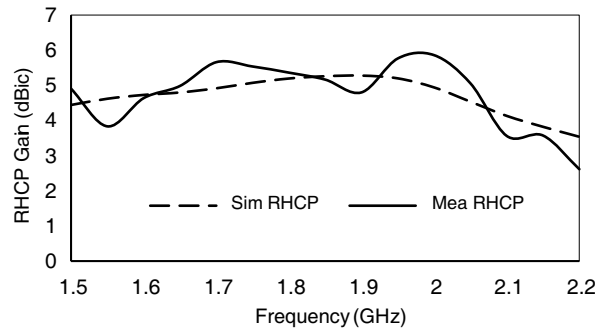


**Figure 9.** RHCP gain of simulated and measured expanded model 3 of ETRS antenna.

Far-field radiation patterns and gain of the fabricated antenna were also measured in an anechoic chamber to confirm simulated results. Fig. 10 shows the measured and simulated far-field radiation patterns of the slotted ETRS antenna when it was radiated by LHCP and RHCP waves in  $x$ - $z$  plane and  $y$ - $z$  plane sequentially. The antenna produces bidirectional radiation with both LHCP and RHCP operations radiated toward  $-z$  direction ( $\theta = 180^\circ$ ) and  $+z$  direction ( $\theta = 0^\circ$ ), respectively. Measured  $x$ - $z$  and  $y$ - $z$  planes far-field radiation patterns at 1.5 GHz, 1.65 GHz, 1.8 GHz, 1.95 GHz and 2.1 GHz show good agreement with the simulated results at the corresponding frequencies. Thus, the proposed antenna offers good CP radiation at both planes. Fig. 9 presents the measured and simulated RHCP gains of the antenna where average gain is around 4.9 dBic with lower gain below 4 dBic found between 2.1–2.2 GHz. It has also been confirmed that both diagonal line slots successfully enhance the gain of ETRS antenna.

Performances and dimension of the measured antenna are compared with those of some related wideband CP printed-slot antennas reported in the literature as tabulated in Table 3. The proposed

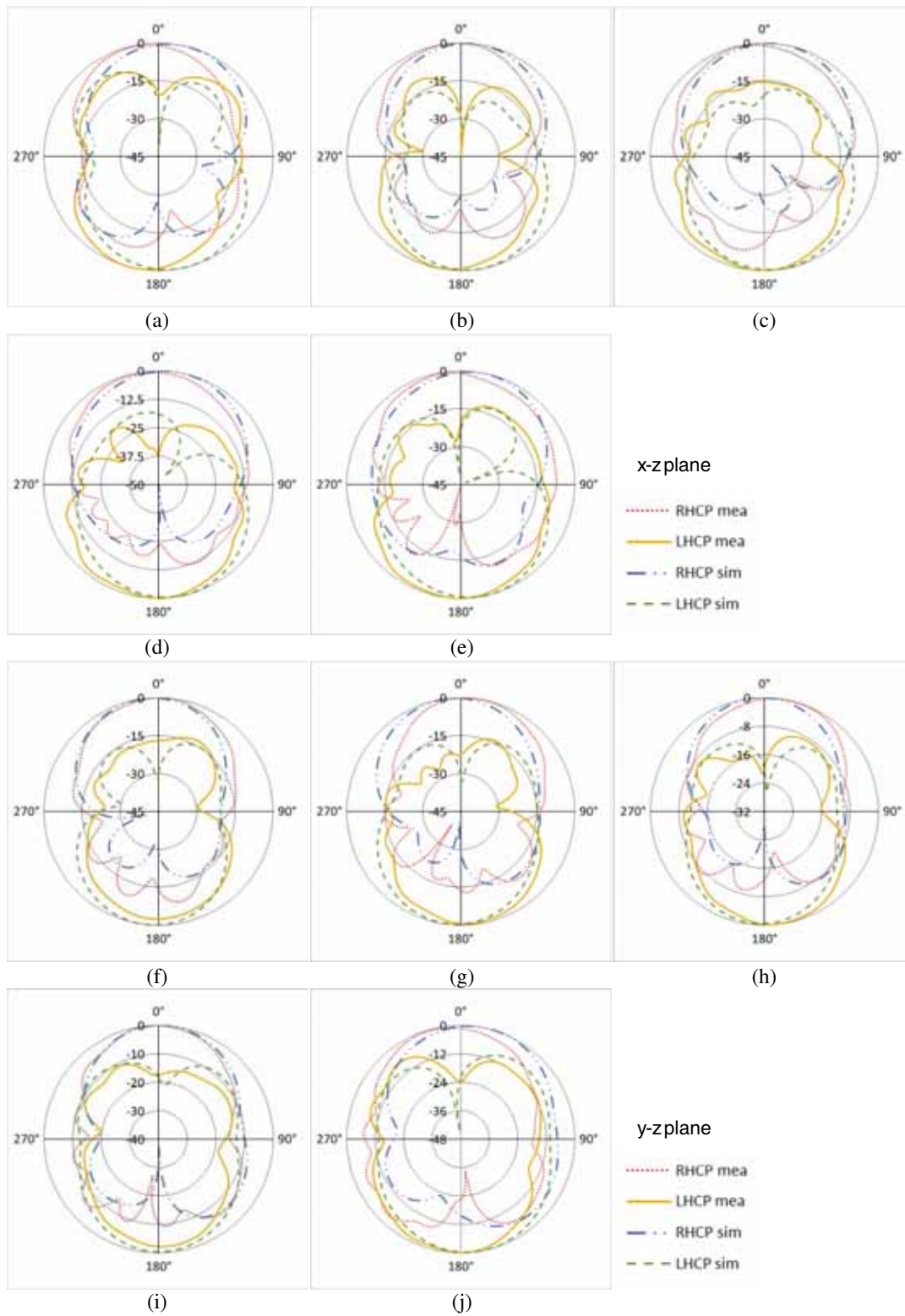


**Figure 10.** Measured and simulated  $x$ - $z$  plane radiation patterns of expanded model 3 ETRS antenna at (a) 1.5 GHz, (b) 1.65 GHz, (c) 1.8 GHz, (d) 1.95, (e) 2.1 GHz, and  $y$ - $z$  plane at (f) 1.5 GHz, (g) 1.65 GHz, (h) 1.8 GHz, (i) 1.95, (j) 2.1 GHz.

**Table 3.** Comparison of CP printed-slot antenna performances.

Ref.	$f_c$ (MHz)	3-dB ARBW (%)	Impedance Bandwidth (%)	Gain (dBic)	Dimension (mm)
[1]	2745	48	51	2.6 to 4.2	$60 \times 60 \times 0.8$
[2]	3625	68	107	3 to 4	$60 \times 60 \times 1.6$
[3]	1590	6.3	14.7	peak 3.6	$54 \times 54 \times 1.6$
[4]	1500	4.3		3.5 to 4.3	$80 \times 80 \times 1.6$
[5]	1638	65	89	3.3 to 5.1	$100 \times 100 \times 0.6$
[6]	2375	12	39	4 to 5.5	$120 \times 120 \times 33$
[7]	3740	44	38	4 to 5	$100 \times 100 \times 1.6$
[8]	3200	31		average 6.7	$100 \times 100 \times 15.1$
Proposed	1840	37	44	3 to 5.8	$150 \times 170 \times 1.6$

ETRS antenna with dual diagonal line slots has broader 3-dB ARBW, lower gain and wider size (but with a different center frequency) than than the antenna with an equilateral triangular wide slot and a parasitic patch [8] which has much thicker dimension. Compared to the other wideband slot antennas without parasitic patch, the proposed antenna has higher peak and average gain.

## 5. CONCLUSION

Polarization of an ETRS antenna can be converted from linear to circular by introducing truncations and perturbation to the slot. However, these introductions yield narrow 3-dB ARBW compared to its impedance bandwidth. Enhancement can be made by inserting two diagonal line slots which have resonant frequency corresponding to the lowest and highest frequencies of an ETRS antenna 3-dB ARBW, respectively. Both diagonal line slots of expanded model 3 have successfully improved 3-dB ARBW by achieving 680 MHz or 37% compared to 254 MHz or 14.7% presented by model 1. It has been confirmed as well that both line slots have improved the gain by model 1. Thus, this design can be implemented for applications which require wideband circularly polarized antenna such as GNSS and satellite communications systems.

## ACKNOWLEDGMENT

This research is supported in part by the Japan Science and Technology Agency (JST) Japan International Cooperation Agency (JICA) FY2010-2016 Science and Technology Research Partnership for Sustainable Development (SATREPS); the European Space Agency (ESA) Earth Observation Category 1 under Grant 6613; the 4th Japan Aerospace Exploration Agency (JAXA) ALOS Research Announcement under Grant 1024; the 6th JAXA ALOS Research Announcement under Grant 3170; the Japanese Government National Budget Ministry of Education and Technology (MEXT) FY2015-2017 under Grant 2101; Chiba University Strategic Priority Research Promotion Program FY2016-FY2018; Taiwan National Space Organization (NSPO); and Indonesian National Institute of Aeronautics and Space (LAPAN).

## REFERENCES

1. Sze, J. Y., C.-I. G. Hsu, Z.-W. Chen, and C.-C. Chang, "Broadband CPW-fed circularly polarized square slot antenna with lightning-shaped feed-line and inverted-L grounded strips," *IEEE Trans. Antennas Propag.*, Vol. 58, No. 3, 973–977, 2010.
2. Nasimuddin, Z.-N. Chen, and X. Qing, "Symmetric-aperture antenna for broadband circular polarization," *IEEE Trans. Antennas Propag.*, Vol. 59, No. 10, 3932–3936, 2011.
3. Row, J. S., "The design of a squarer-ring slot antenna for circular polarization," *IEEE Trans. Antennas Propag.*, Vol. 53, No. 6, 1967–1972, 2005.

4. Wong, K. L., C. C. Huang, and W. S. Chen, "Printed ring slot antenna for circular polarization," *IEEE Trans. Antennas Propag.*, Vol. 50, No. 1, 75–77, 2002.
5. Sze, J. Y. and W. H. Chen, "Axial-ratio-bandwidth enhancement of a microstrip-line-fed circularly polarized annular-ring slot antenna," *IEEE Trans. Antennas Propag.*, Vol. 59, No. 7, 2450–2456, 2011.
6. Wong, K. L., J. Y. Wu, and C. K. Wu, "A circular-polarized patch loaded square slot antenna," *Microw. Opt. Technol. Lett.*, Vol. 23, No. 6, 363–365, 1999.
7. Tseng, L. Y. and T. Y. Han, "Microstrip-fed circular slot antenna for circular polarization," *Microw. Opt. Technol. Lett.*, Vol. 50, No. 4, 1056–1058, 2008.
8. Han, T. Y., Y. Y. Chu, L. Y. Tseng, and J. S. Row, "Unidirectional circularly-polarized slot antennas with broadband operation," *IEEE Trans. Antennas Propag.*, Vol. 56, No. 6, 1777–1780, 2008.
9. Chang, T. N. and J. M. Lin, "Circularly polarized antenna having two linked slot-rings," *IEEE Trans. Antennas Propag.*, Vol. 59, No. 8, 3057–3060, 2011.
10. Zhang, J. L. and X. Q. Yang, "Integrated compact circular polarization annular ring slot antenna design for RFID reader," *Progress In Electromagnetics Research Letters*, Vol. 39, 133–140, 2013.
11. Qing, X. M. and Y. W. M. Chia, "Circularly polarized circular ring slot antenna fed by stripline hybrid coupler," *Electronics Letters*, Vol. 35, No. 25, 2154–2155, 1999.
12. Sharma, C. and K. C. Gupta, "Analysis and optimized design of single feed circularly polarized microstrip antennas," *IEEE Trans. Antennas Propag.*, Vol. 31, No. 6, 949–955, 1983.
13. Lu, H. J., C. L. Tang, and K. L. Wong, "Single-feed slotted equilateral-triangular microstrip antenna for circular polarization," *IEEE Trans. Antennas Propag.*, Vol. 47, No. 7, 1174–1178, 1999.
14. Aziz, M. Z. A. A., N. A. D. A. Mufit, M. K. A. Rahim, and M. R. Kamaruddin, "Design X-circular polarized with slant rectangular slot by using single port," *2012 International Symposium on Antennas and Propagation.*, 555–558, 2012.
15. Rafi, G. Z. and L. Shafai, "Low-cross-polarized wideband V-slot microstrip antenna," *Microwave and Optical Technology Letters*, Vol. 43, No. 1, 44–47, 2004.
16. Ortego, I. M., M. S. Perez, M. Zhang, J. Hirokawa, and M. Ando, "Mutual coupling in longitudinal arrays of compound slots," *Progress In Electromagnetics Research B.*, Vol. 46, No. 46, 59–78, 2013.
17. Behdad, N. and K. Sarabandi, "A wide-band slot antenna design employing a fictitious slot circuit concept," *IEEE Trans. Antennas Propag.*, Vol. 53, No. 1, 475–482, 2005.
18. Mazzarella, G. and G. Panariello, "On the evaluation of mutual coupling between slots," *IEEE Trans. Antennas Propag.*, Vol. 35, No. 11, 1289–1293, 1987.